Supplemental Materials

Methods and Materials

Sample:

Participants were recruited from an epidemiological cohort (N=752) and were selected according to: a) their age (12-16 years of age), and b) family status of substance used disorder (DSM-IV; parental SUD diagnosis is referred to as FH+, no parental SUD diagnosis is referred to as FH-). Of the epidemiological cohort, 242 children who were eligible to participate in the study based on the above criteria, were contacted via letters for recruitment. One week after the letters were mailed, recruiters followed up with the families via telephone and in-person visits. Families were initially scheduled for a screening interview to determine the child's eligibility to participate in the MRI portion of the study. A child and at least one parent of 153 families completed the screening interview, and 125 agreed to participate in the fMRI study. Participating subjects drawn from the eligible subsample were similar to those that did not participate, as they did not differ by gender, race/ethnicity, household income, FH status, and BIS-11 (Patton, Stanford, & Barratt, 1995) and STAI (Spielberger, Gorsuch, Lushene, Vagg, & Jacobs, 1983) sub-scales (all p-values >0.15). Non-participants were on average 0.7 years older than participants (p=0.03). Family SUD status was determined based on lifetime and past year alcohol/drug use or dependence of biological mother and/or father using the Composite International Diagnostic Interview (CIDI) assessed on two previous waves and during the screening prior to the current study. Based on these criteria, 60 adolescents (mean age 14.98±1.29) were classified as controls (FH-), and 65 (mean age 15.11±1.36) were classified as having parental SUD (FH+). Based on substance used assessments, the adolescents themselves had very limited substance exposure.

Of the 124 MRI study participants, data from only 102 were included in the imaging analysis (for exclusion reasons, see the paper). These 102 participants consisted of 53 FH+ (mean age 15.2±1.4) and 49 FH-(mean age 15.1±1.3). Table S1 and S2 present the demographic, impulsivity (BIS 11) and anxiety measures (STAI) by their FH status. As in the full sample (N=125), these FH+ and FH- subgroups did not differ in any demographic, anxiety or impulsivity measures.

Table S1: Demographic Information and Comparison of the FH+ and FH- Groups for N=102

	FH+ (N=53) N (%)	FH- (N=49) N (%)	Chi-square	df	P	N missing
Female	28 (52.83)	25 (51.02)	0.03	1	0.86	0
SES (household income)						
<$15K	16 (32.00)	18(39.13)	1.29	2	0.52	6
$15-50K	22 (44.00)	21(45.65)				
>$50K	12 (24.00)	7 (15.22)				
Ethnicity						
Hispanic	32 (60.38)	32 (65.31)	0.30	2	0.86	0
Black	13 (24.53)	11 (22.45)				
Other	8 (15.09)	6 (12.24)				

Table S2: Impulsivity and Anxiety Measures Comparison of the FH+ and FH- Groups for N=102

	FH+ (N=53)	FH- (N=49)	T -test	df	P	N missing
	Mean (SD)	Mean (SD)				
BIS 11						
Attentional impulsiveness	16.58 (3.39)	15.60 (2.71)	-1.60	98	0.11	2
Motor impulsiveness	21.77 (4.47)	21.17 (3.65)	-0.74	98	0.46	2
Non-planning impulsiveness	28.09 (5.28)	27.06 (4.92)	-1.01	99	0.31	1
STAI						
State	35.03 (8.83)	32.31 (8.41)	-1.58	99	0.12	1
Trait	36.83 (9.36)	35.60 (8.85)	-0.68	98	0.50	2

Data analysis:

Prior to the reported analyses, we explored both the behavioral and the fMRI data on a subset of participants. We tried to calculate the subjective value parameter (k) for each participant but that was not feasible because we could not consistently calculate the indifference points for a large number of participants who chose almost exclusively SS or LL. For the same reason, our fMRI choice-based analysis excluded many participants. To include as many participants as possible in the analysis, we decided to conduct an option-based analysis as reported in the paper.

Behavioral

Initially, we included all subjects' data for the behavioral analysis as reported in the paper. We repeated the same behavioral analytical models for the two subsamples (N=102 and N=89) used in the neuroimaging analysis (see Results section below). The data were analyzed at the trial level without aggregation. Trials with missing responses or with reaction time < 200 ms were not included, but these were rare occurrences. The primary dependent variable was the choice participants made for each trial (SS or LL). The compiled trial-by-trial choice data were submitted to statistical analysis using Bayesian generalized linear mixed-effects models in R using the brms package (Bürkner, 2017) which provides an interface to Stan (Carpenter et al., 2017). Stan is a state-of-the-art platform for Bayesian data analysis that can be modeled via R. The model included predictors that represented main effects of Group, Immediacy (Now/Not-Now), Frame (Delay/Acceleration), Time Difference, SS Reward, and Relative Reward Difference (RRD). In addition, the model included the interaction of each of these factors with Group, except for the SS Reward. The continuous predictors (SS Reward, RRD) were mean-centered and standardized. All categorical predictors (Group, Now/Not-now, Time Difference, Frame) were coded using sum-to-zero contrasts. To account for the repeated-measures nature of the data, the model included a random intercept for each participant, random slopes

varying over participants for each of the within-subject predictors, and all possible pairwise covariances between random effects. The model was fit using six chains with 2,000 iterations each (1,000 warm up), and was inspected for convergence via the Rhat values and visual inspection of the trace plots. All primary results are derived from this model. Coefficients were deemed statistically significant if the associated 95% posterior credible intervals were non-overlapping with zero.

Neuroimaging

fMRI data were pre-processed using SPM12 (Wellcome Department of Imaging Neuroscience, London, UK; see http://www.fil.ion.ucl.ac.uk/spm/spm12.html) implemented in Matlab R2018a (Mathworks, Inc., Natick, MA). The first five volumes were excluded at the time of acquisition to allow for signal stability following onset transients. Data were corrected for differences in slice timing with respect to the first slice. Images were realigned with respect to the mean volume, normalized to the MNI template space, resampled at 2 x 2 x 2 mm, and smoothed with a Gaussian kernel of 8 mm^3 (Friston et al., 1995). Scan-to-scan motions greater than 2mm were detected using the ArtRepair toolbox (Mazaika, Hoeft, Glover, & Reiss, 2009) and scrubbed from future analysis using null regressors. Imaging runs with more than 10% of unusable volumes were excluded from the analysis. The average frame displacement (FD) was similar between groups (FH+ FD mean (SD)= 0.50 (0.23); FH- FD mean (SD)= 0.54 (0.29); p= 0.479**).** A 128-seconds temporal high-pass filter was applied to the data to remove low-frequency noise. For choice-based GLM2 (N=89), we included subjects who had at least 10 trials (15%) for each regressor. Both groups had a similar number of SS choices during the Now and Not-Now trials as well as similar LL choices during the Now and Not-Now trials, as shown in Table S3.

Table S3: Mean numbers of choices (mean and range) for each group that were used in the GLM2.

	Choices	**SS**		**LL**	
	Trial Types	**Now**	**Not -Now**	**Now**	**Not -Now**
FH-	**Mean (SD)**	48.70 (13.84)	50.89 (15.23)	24.20 (13.17)	22.48 (15.19)
	Range	16 - 82	12 -72	3 - 55	1 - 54
FH+	**Mean (SD)**	53.28 (17.40)	49.95 (17.78)	21.13 (15.98)	24.48 (18.74)
	Range	18 - 86	16 - 80	2 - 60	5 - 62
FH-/FH+	**t-test**	**0.086**	**0.395**	**0.076**	**0.407**

Results

Behavioral

Tables S4A and S4B presents the regression coefficients and the confidence intervals for the behavioral performance in the DD task using the Bayesian mixed effects model for the subsamples of N=102 and N=89 participants respectively. For both subsamples, there were significant interactions between Group and the Now/Not-Now and between Group and RRD factors. Figures S1A and S1B demonstrate the Group by trial types interaction. In the Now trials, the group difference was driven by the FH+ participant choosing LL less often (SS more often) than the FH- participants. Note that the analyses of the N=124, N=102 and N=89 were consistent in that only the FH+ group exhibited an immediacy effect (sometimes referred as present bias or now effect) (Figner et al., 2010; Prelec & Loewenstein, 1991). The immediacy effect supports the notion that more self-control is required to make LL choices in the presence of immediate rewards.

In Not-Now trials, proportion of LL choices were similar for the FH+ and FH- in the full sample as well as in the N=89 subsample. However, in the N=102 subsample, the FH- participants chose LL less often than the FH+ participants. These results were initially unexpected as one might expect that the FH- would make a similar proportion of LL choices in both the Now and Not-Now trials. We provided a possible explanation in the paper, suggesting that the FH- group who are future oriented and were willing to wait for later reward, were more sensitive to the additional delay in the Not-Now trials. Therefore, the FH- participants may become less patient in the Not-Now trials and preferred an earlier reward. For the FH- group, the two trial types were not equivalent as the participants were more sensitive to variability in time delay than the FH+ participants which were more sensitive to immediacy.

Participants were more likely to choose LL as RRD increased. The RRD factor also interacted with Group indicating that groups differed in their choices as a function of relative difference between the SS and LL reward options. Figure S2A and S2B for the N=102 and for the N=89 subsamples, respectively, show that for both FH groups as RRD increases there was an increase in LL choices. However, this increase in LL choices was significantly smaller in the FH+ compare to the FH- group, also supporting more impulsive behavior among the FH+ participants.

Only in the subsample of N=89 was there a significant interaction of Group and Frame demonstrating that the FH+ and FH- groups differed in the proportion of LL choice in the delay and acceleration conditions. There is evidence in the literature that the default presentation affects people's decisions (Weber et al., 2007). Figure S3 shows that FH+ participants chose LL infrequently for both delayed and accelerated conditions, and they were consistent in their preference for immediate rewards. In contrast, the FH- participants were more sensitive to the condition manipulation and as expected made more LL choices in the accelerated than the delayed condition.

Table S4A: Bayesian Model Results for the Behavioral Performance in the DD (N=102)

Variables	B Estimate	Est. Error	l-95% CI	U-95% CI
SS Reward[a]	0.756	0.071	0.617	0.900
Now/Not-Now[a]	-0.404	0.157	-0.717	-0.097
Relative Reward Differences (RRD) [a]	1.063	0.105	0.859	1.276
Time Difference[a]	-0.729	0.126	-0.982	-0.487
Frame	0.244	0.127	-0.004	0.500
Group	-0.290	0.358	-0.995	0.405
Now/Not-Now by Group[a]	0.566	0.211	0.146	0.987
RRD by Group[a]	-0.280	0.117	-0.514	-0.048
Time Difference by Group	0.212	0.170	-0.123	0.550
Frame by Group	-0.239	0.177	-0.590	0.108

[a] P< 0.05

Table S4B: Bayesian Model Results for the Behavioral Performance in the DD (N=89)

Variables	B Estimate	Est. Error	l-95% CI	U-95% CI
SS Reward[a]	0.807	0.075	0.659	0.955
Now/Not-Now[a]	-0.436	0.160	-0.750	-0.122
Relative Reward Differences (RRD) [a]	1.066	0.111	0.885	1.325
Time Difference[a]	-0.721	0.128	-0.975	-0.472
Frame[a]	0.263	0.120	-0.025	0.502
Group	-0.412	0.329	-1.062	0.225
Now/Not-Now by Group[a]	0.583	0.228	0.130	1.043
RRD by Group[a]	-0.306	0.124	-0.542	-0.060
Time Difference by Group	0.166	0.180	-0.189	0.526
Frame by Group[a]	-0.387	0.166	-0.718	0.065

[a] P< 0.05

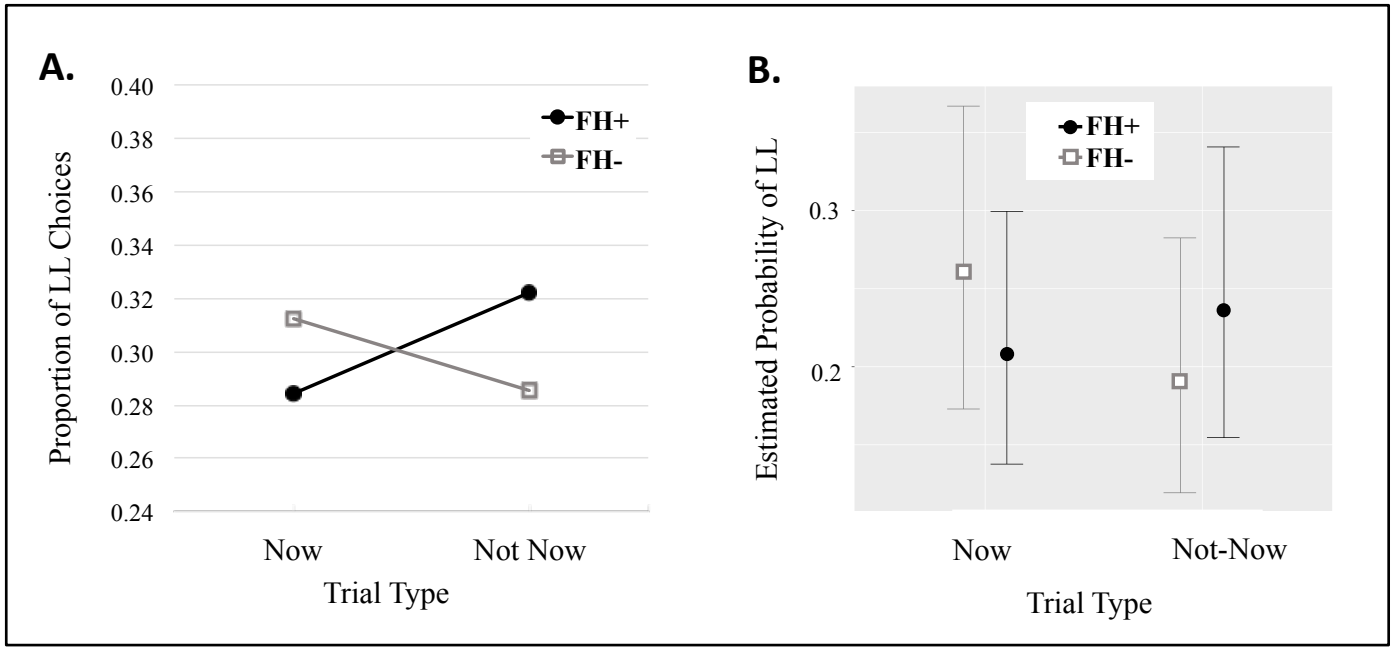

Figure S1A: Proportion of LL choices for the Now and Not-Now trials for the FH+ and FH- groups (N=102). A. represents the choice proportions computed from the raw data. B. represents the estimated marginal mean probabilities based on the Bayesian model (with 95% CIs).

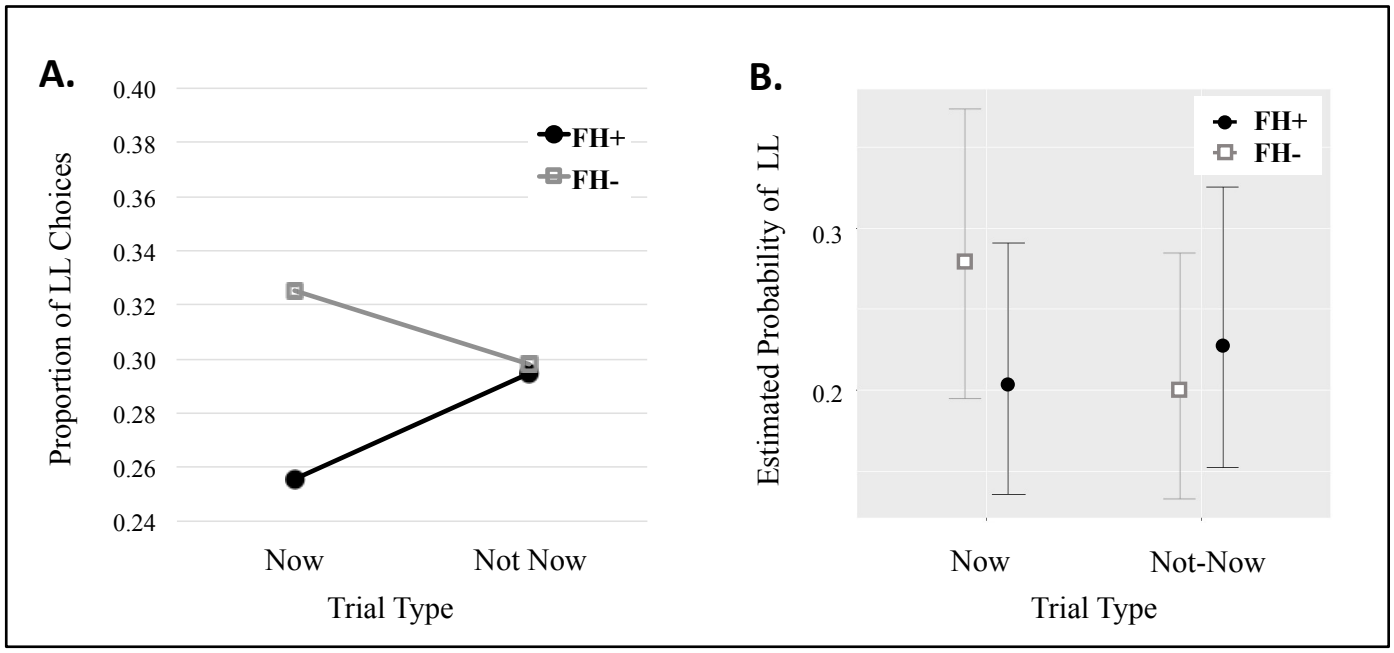

Figure S1B: Proportion of LL choices for the Now and Not-Now trials for the FH+ and FH- groups (N=89). A. represents the choice proportions computed from the raw data. B. represents the estimated marginal mean probabilities based on the Bayesian model (with 95% CIs).

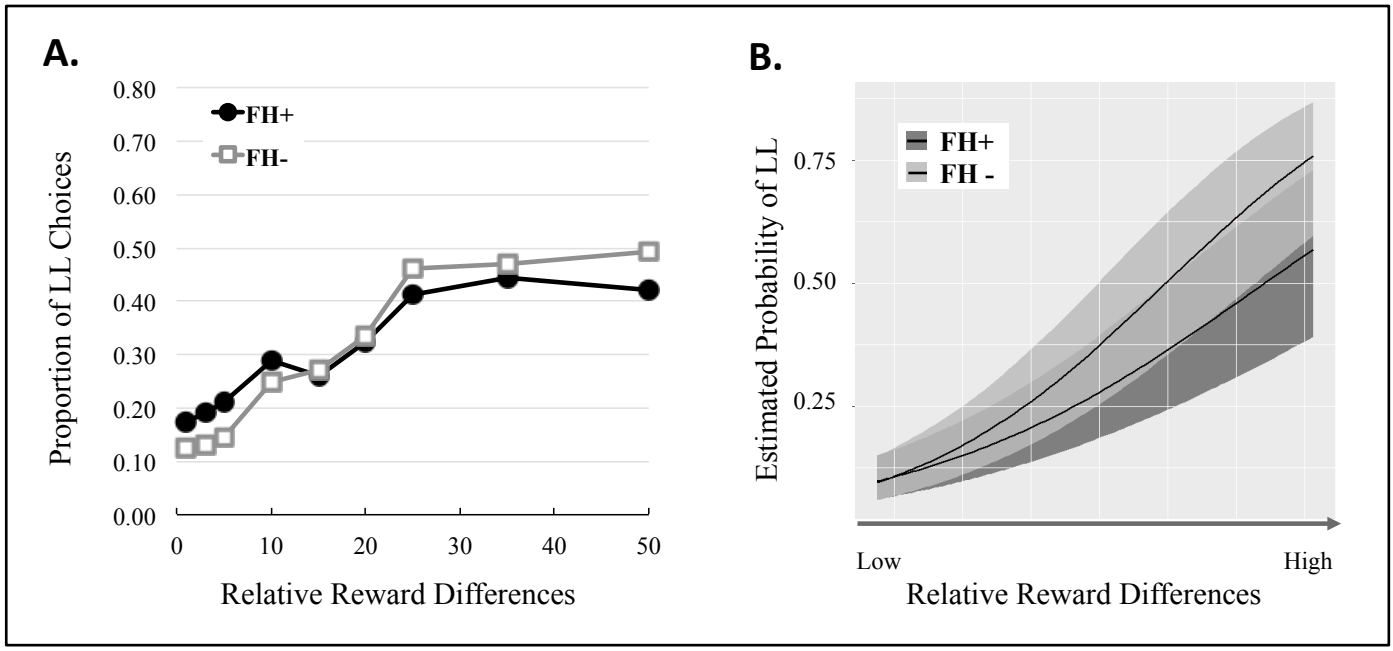

Figure S2A: The proportion of LL choices as a function of the RRD for the FH+ and FH- groups (N=102). A. represents the choice proportions computed from the raw data. B. represents the estimated marginal mean probabilities based on the Bayesian model (with 95% CIs).

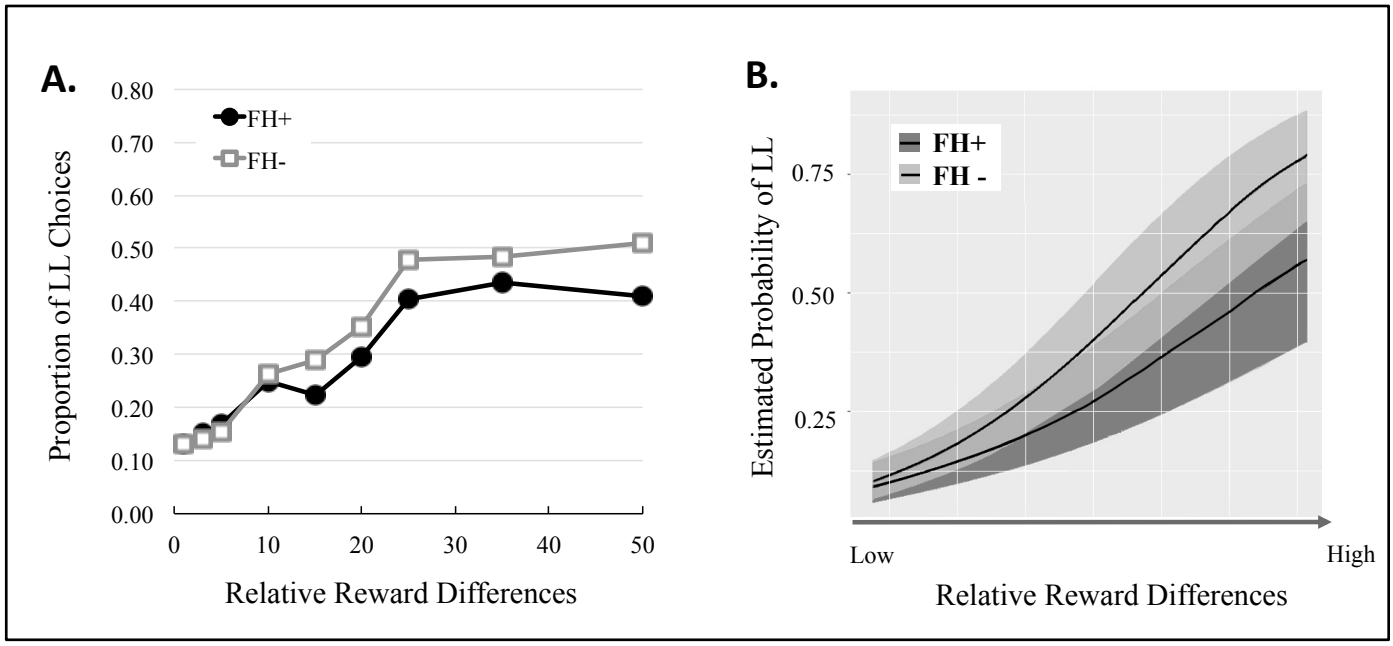

Figure S2B: The proportion of LL choices as a function of the RRD for the FH+ and FH- groups (N=89). A. represents the choice proportions computed from the raw data. B. represents the estimated marginal mean probabilities based on the Bayesian model (with 95% CIs).

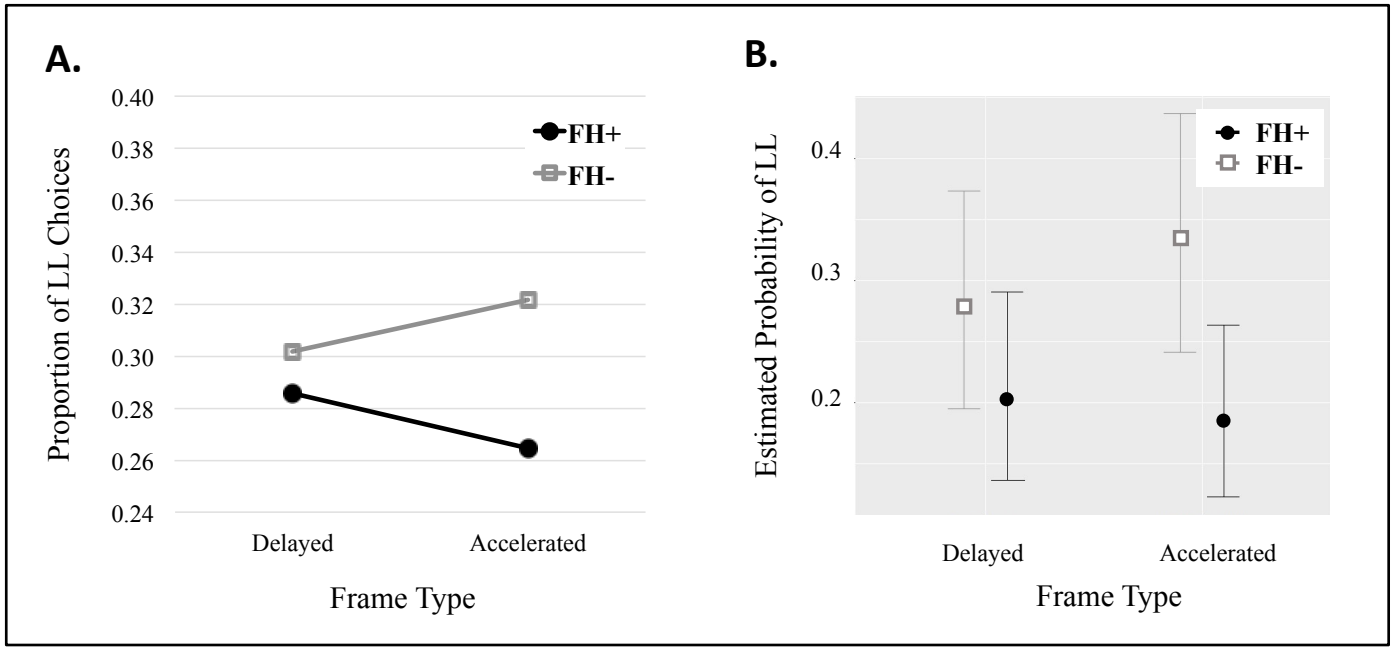

Figure S3: The proportion of LL choices as a function of Frame (delay and acceleration) for the FH+ and FH- groups (N=89). A. represents the choice proportions computed from the raw data. B. represents the estimated marginal mean probabilities based on the Bayesian model (with 95% CIs).

Neuroimaging

Investigation of reward processing network during the DD task (uncorrected results)

Our main imaging findings for the immediacy effect (Now vs Not-Now trials) in the paper demonstrated the engagement of previously described decision-making regions. However, the VS, which has been associated with reward processing, were only observed at uncorrected thresholds ($P < 0.005$ voxel-level and cluster size > 50 voxels) for the option-based analysis but not for the choice-based analysis (Figure S4 A and B). Tables S5A and S5B show all the regions observed for the option-based analysis (GLM1) and the choice-based analysis (GLM2). These uncorrected findings are in line with our interpretation that the option-based analysis reflects the decision process while the choice-based analysis is more associated to the preparation for choice selection.

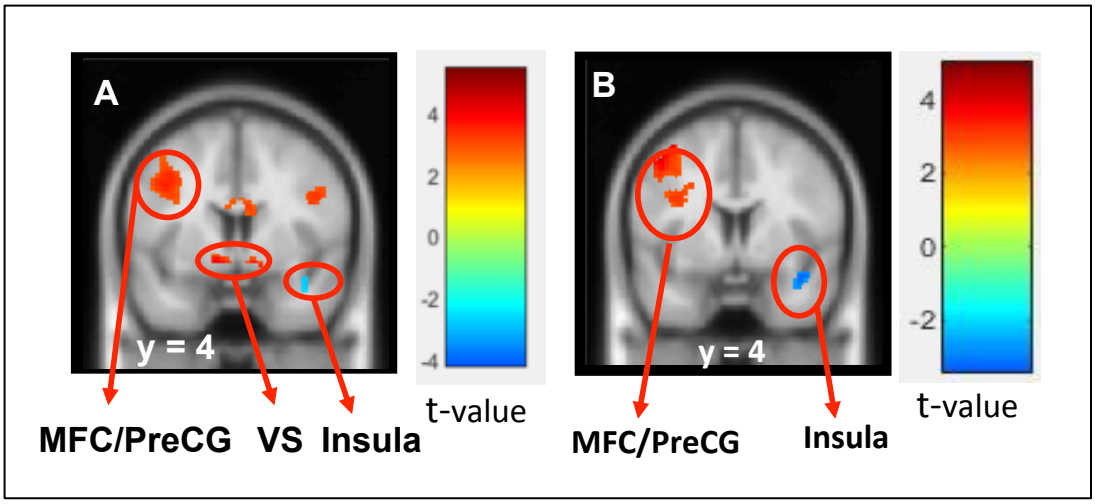

Figure S4: Group random-effects results comparing Now vs. Not-Now for FH- and FH+ groups combined for A. the GLM1 (N=102) and B. the GLM2 (N=89). Maps are threshold at p-unc<0.005 at the voxel level and a spatial extent of 50.

Table S5A: Brain regions active for the contrast of Now > Not-Now trials for the combined groups in the option-based analysis (GLM1)

	Brain Regions	Brodmann Area	Peak *t*-value	Cluster size	MNI Coordinates		
					x	y	z
NOW > NOT NOW							
L/R	Temporal (MTG, pHIPP)	37	5.40	14990	-44	-56	-14
	Occipital (MOG,FUS, IOG)	19					
	Parietal (PCC, Pcu)	31, 7					
L	Frontal (IFG, PreCG, MFG)	9, 6, 46, 45	4.53	1316	-48	26	14
L/R	Frontal (ACC/mPFG, SFG, mOFC)	10, 32, 9, 24	4.40	2659	-10	40	10
R	Frontal (MFG, IFG)	46, 9	4.37	918	34	22	24
	Limbic (Insula)	13					
L/R	Striatum (Gl. Pallidus, Caudate)		4.13	202	10	2	-10
R	Frontal (mSFG, SFG)	6	3.36	66	10	40	40
L/R	Frontal (MCC)	24	3.31	77	8	6	24
NOT NOW > NOW							
R	Frontal (PreCG, MCC, SMA)	31, 6	-4.21	72	10	-20	50
R	Temporal (STG)		-3.47	51	40	0	-20
	Limbic (Insula)						

P < 0.005 uncorrected and cluster size threshold of 50 voxels

Table S5B: Brain regions active for the contrast of SS Now choices > SS Not-Now choices for the combined groups for the choice-based analysis (GLM2)

	Brain Regions	Brodmann Area	Peak *t*-value	Cluster size	MNI Coordinates x	y	z
NOW > NOT NOW							
L	Temporal (ITG, MTG, STG)	21, 22, 37,	5.02	6674	-42	-60	-8
	Occipital (IOG, FUS)	19					
R/L	Parietal (Pcu, PCC)	7, 39, 40, 23, 30,					
R	Temporal (MOG, SOG)	39,31	4.75	930	42	-80	-10
	Occipital (IOG, FUS, LG)	17, 18, 19					
L	Frontal (MFG, IFG, PreCG)	6, 7, 8, 44, 45, 46	4.43	1311	-44	8	52
R	Frontal (MFG, SFG)	8, 9	4.35	914	26	30	54
R	Temporal (ITG, MTG, FUS)	37, 20, 21	4.21	1159	38	-44	-28
	Cerebellum						
R	Frontal (MFG, IFG, PreCG)	9, 45, 46	4.00	481	54	26	16
L	Frontal (SFG, MFG)	8, 9, 32, 6	3.93	599	-26	32	50
L	Limbic (HIPP, pHIPP, AMY)	38	3.83	52	-12	-14	-18
R/L	Frontal (MFG)	10	3.77	350	0	64	12
R	Parietal (ANG, SPL, Pcu)	39, 40,	3.56	195	50	-62	40
	Occipital (MOG, SOG)	-					
	Temporal (MTG)	22					
R	Parietal (ANG, SPL)	7, 40	3.37	188	38	-60	52
	Occipital (SOG)	-					
R/L	Frontal (mSFG, ACC)	9, 10, 32	3.29	113	2	50	20
L	Frontal (PreCG)	3, 2	3.23	63	-40	-26	46
	Parietal (PostCG, SMG)	40					
NOT NOW > NOW							
R	Limbic (Insula, Hipp)		-3.39	53	40	2	-18
	Temporal (STG)	38					

P < 0.005 uncorrected and cluster size threshold of 50 voxels

Abbreviations: L, left; R, right; MTG, middle temporal gyrus; pHIPP, para hippocampal gyrus; MOG, middle occipital gyrus; FUS, fusiform gyrus; IOG, inferior occipital gyrus; PCC, posterior cingulate gyrus; Pcu, precuneus; IFG, inferior frontal gyrus; PreCG, precentral gyrus; MFG, middle frontal gyrus; ACC, anterior cingulate gyrus; mPFC, medial prefrontal cortex; SFG, superior frontal gyrus; mOFC, medial orbitofrontal cortex; mSFG, medial superior frontal gyrus; MCC, middle cingulate gyrus; SMA, supplementary motor area; STG, superior temporal gyrus; ITG, inferior temporal gyrus; SOG, superior occipital gyrus; LG, lingual gyrus; HIPP, hippocampus; AMY, amygdala; PostCG, postcentral gyrus.

Option-based analysis for each Group Separately

Our main imaging findings show that there were no group differences in brain activity when comparing Now and Not-Now trials, but there was a widespread network of regions related to the decision-making in the combined groups results. To aid in the interpretation of these findings, we assessed subthreshold activations associated with the immediacy effect in both groups. Specifically, we expected to observe activation in striatal regions because of its involvement in reward processing. The brain activity comparisons between Now vs. Not-Now trials for each group are shown in Figure S5 and Table S6. For the FH- group, brain activity for this contrast was observed in the medial OFC, ACC/mPFC, precuneus, PCC, inferior-, middle- and superior-frontal gyrus, temporal gyrus and occipital gyrus. In contrast, brain activity comparison for the FH+ group show activation in the occipital, temporal and parietal regions. These findings suggest that the observed pattern of activation in reward circuitry during the DD task for the combined groups, reported in the paper (Figure 4), was contributed mostly by the differential activation between Now and Not-Now trials in the FH- group. This is somewhat surprising as we expected activity in that region for both groups. One possible explanation is that the FH+ participants who were more impulsive did not engaged valuation regions as they made their choices for the immediate reward. In contrast, the FH- participants made their choices based on their assessment of the reward values and the delivery time, and thus demonstrated clear activity in the reward network.

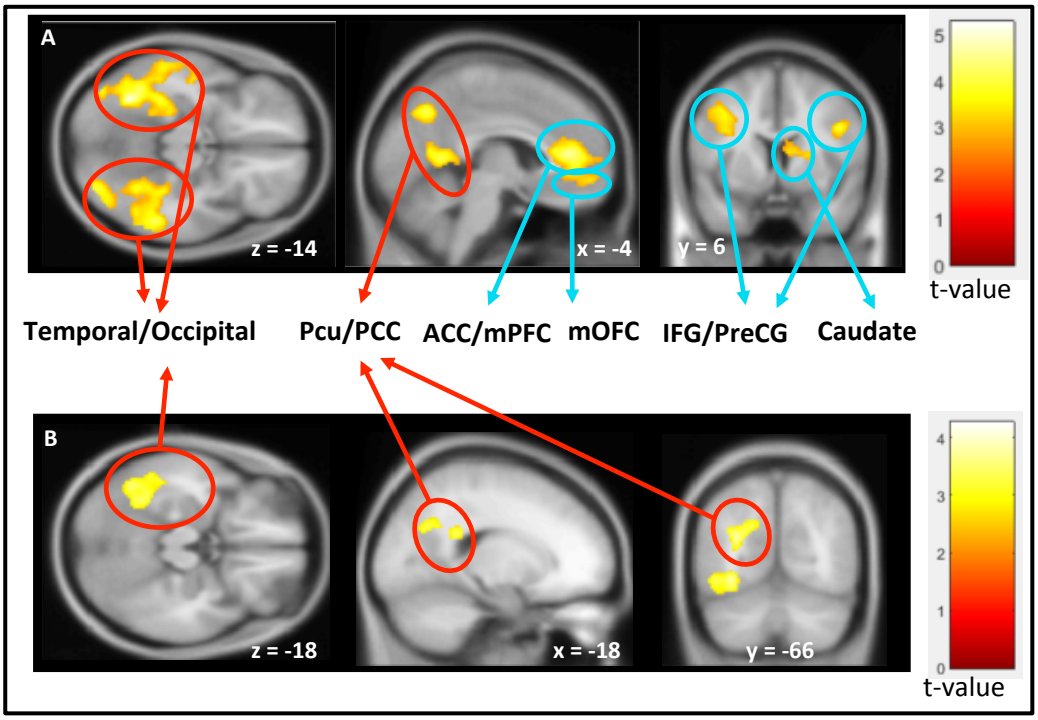

Figure S5: Group random-effects results comparing Now vs. Not-Now for the FH- group (A) and for the FH+ group (B) (N=102). Maps are threshold at p<0.05 FPR corrected (voxel-level uncorrected p<0.005 and cluster size threshold of 1074 voxels in panel A, and 830 voxels in panel B). Red circles indicate areas active in both groups, while blue circles indicate areas active only on FH+.

Table S6: Results for the contrast of Now > Not-Now trials for the FH- and the FH+ groups separately.

Brain Regions		Brodmann Area	Peak *t*-value	Cluster size	MNI Coordinates x	y	z
FH- Now > Not-Now trials							
L	Temporal (ITG)	20, 21, 22	5.27	5256	-40	-48	-22
	Limbic (pHIPP)	36, 37					
	Occipital (LG, FUS)	18, 19					
L/R	Parietal (Pcu)	7, 39, 23, 29, 30, 31					
	Cerebellum						
R	Temporal (ITG)	20, 39	4.57	2156	38	-38	-18
	Occipital (LG, FUS)	18, 19					
L/R.	Frontal (OFC, ACC/mPFC)	9, 10, 32, 24	4.74	2904	8	46	12
L	Frontal (IFG, PreCG)	9, 46, 45, 6	4.98	1209	-46	28	14
R	Frontal (IFG, PreCG)	9, 46, 6	4.44	1079	36	18	20
	Limbic (Insula)	13					
	Striatum (Caudate)						
FH+ Now > Not-Now trials							
L	Occipital (FUS, SOG)	18, 19	4.26	2010	-44	-60	-10
	Temporal (ITG, MTG)	20, 37					
L	Parietal (Pcu, PCC)	31, 23, 30	3.90	803	-6	-44	24

P < 0.05 FPR cluster-level corrected (voxel level P < 0.005 and a cluster size > 987 voxels for FH- and 500 voxels for FH+)

Abbreviations: ITG, inferior temporal gyrus; pHIPP, parahippocampal gyrus; LG, lingual gyrus; FUS, fusiform gyrus, Pcu, precuneus; OFC, orbitofrontal cortex; ACC, anterior cingulate cortex; mPFC, medial prefronatl cortex, IFG, inferior frontal gyrus; PreCG, precentral gyrus; SOG; superior occipital gyrus; MTG, middle temporal gyrus: PCC, precuneus

References

Bürkner, P.-C. (2017). Advanced Bayesian multilevel modeling with the R package brms. *arXiv preprint arXiv:1705.11123*.

Carpenter, B., Gelman, A., Hoffman, M. D., Lee, D., Goodrich, B., Betancourt, M., . . . Riddell, A. (2017). Stan: A probabilistic programming language. *Journal of statistical software, 76*(1).

Figner, B., Knoch, D., Johnson, E. J., Krosch, A. R., Lisanby, S. H., Fehr, E., & Weber, E. U. (2010). Lateral prefrontal cortex and self-control in intertemporal choice. *Nat Neurosci, 13*(5), 538-539.

Friston, K. J., Holmes, A. P., Worsley, K. J., Poline, J. B., Frith, C. D., & Frackowiak, R. S. (1995). Statistical parametric maps in functional imaging: a general linear approach. *Human brain mapping, 2*, 189—210.

Mazaika, P. K., Hoeft, F., Glover, G. H., & Reiss, A. L. (2009). Methods and software for fMRI analysis of clinical subjects. *Neuroimage, 47*(Suppl 1), S58.

Patton, J. H., Stanford, M. S., & Barratt, E. S. (1995). Factor structure of the Barratt impulsiveness scale. *J Clin Psychol, 51*(6), 768-774.

Prelec, D., & Loewenstein, G. (1991). Decision making over time and under uncertainty: A common approach. *Management Science, 37*(7), 770-786.

Spielberger, C. D., Gorsuch, R. L., Lushene, R., Vagg, P. R., & Jacobs, G. A. (1983). *Manual for the State-Trait Anxiety Inventory*. Palo Alto, CA: Consulting Psychologists Press.

Weber, E. U., Johnson, E. J., Milch, K. F., Chang, H., Brodscholl, J. C., & Goldstein, D. G. (2007). Asymmetric discounting in intertemporal choice: a query-theory account. *Psychol Sci, 18*(6), 516-523.